ELSEVIER

Carbohydrate Polymers 36 (1998) 205–216

Carbohydrate Polymers

Physico-chemical characterization of chitosans varying in degree of acetylation

Gisela Berth[a,*], Herbert Dautzenberg[b], Martin G. Peter[a]

[a]*Universität Potsdam, Institut für Organische Chemie und Strukturanalytik, D-14469 Potsdam, Germany*
[b]*Max-Planck-Institut für Kolloid- und Grenzflächenforschung, D-14513 Teltow, Germany*

Received 18 July 1997; revised 4 November 1997; accepted 17 December 1997

Abstract

Three commercial chitosans varying in average degree of acetylation (DA) were characterized in terms of average molar masses M_n, M_w, the second virial coefficient B and radius of gyration $R_{g,z}$, and intrinsic viscosities by membrane osmometry, static light scattering, and capillary viscometry in acetate buffer of pH 4.5. To obtain satisfactory light scattering data, the method used for clarification was of great importance. Combined ultracentrifugation and membrane filtration was found to be the method of choice. Using the model for wormlike chains with excluded volume and a logarithmic molar mass distribution, the persistence length L_P was determined as $L_P = 6$ nm. No concentration-dependent association was observed for the low concentrations studied. Samples were also fractionated on Sepharose CL-2B for subsequent light scattering and viscosity measurements to establish relationships between M_w and $[\eta]$ and R_g, respectively. These relationships were found to be independent of the DA for the bulk of molecularly dispersed chitosan. Model calculations aimed at checking the consistency of data led, as to be expected, to an increasing excluded volume effect with increasing molar mass and steadily increasing polydispersities of the fractions with increasing elution volume. The levelling off of the $[\eta]$–M_w and R_g–M_w relations for fractions of increasingly high molar mass was assigned to chemical heterogeneity of samples in terms of DA distributions.

Keywords: Chitosan; Macromolecular characterization; Wormlike chain model; Mark–Houwink equation; Static light scattering

1. Introduction

There is a steadily expanding market for chitosans which are used especially in cosmetics and pharmaceuticals (Peter, 1995). For example, the use of chitosan for the production of biocompatible microcapsules is under study (Hunkeler, 1997). Stimulated by these developments, there is also a growing academic interest in the molecular architecture of chitosans. Knowing the architecture and the effects which govern the behaviour of molecules in solution may well help to improve our understanding of what kind of role these species play in their natural environment or in man-made composites.

The chemical structure has been ascertained with the help of methods for the determination of the average degree of acetylation (DA) and the distribution of acetyl group along the linear copolymer. In contrast, a lot of contradicting results have been published on the conformation. A central point of the current debate is whether or not a varying degree of acetylation causes any changes in the expansion and stiffness of the chains or the tendency to aggregate (Ottøy et al., 1996b). Two effects have to be considered. On the one hand, a higher content of bulky acetyl groups may increase the stiffness of the chains for steric reasons. On the other hand, a lower DA means automatically a higher amount of amino groups. In acidic solution, the latter bind protons so that, finally, a highly charged polycation is formed. It is known that, in the case of flexible polymer chains, the accumulation of charges leads to considerable expansion due to electrostatic repulsion. This effect is most important at very low ionic strengths. At high ionic strengths, repulsion is largely suppressed due to the screening effect of the added salt. Then the electrostatic contribution to chain stiffness becomes small. For this reason, a high ionic strength is desirable for the characterization of polyelectrolytes in terms of molecular parameters.

There is full agreement that chitosans form single-stranded stiff chains in acidic aqueous solution. Whereas the Trondheim group has obtained a lot of evidence for a

* Corresponding author: MPI for Colloids and Interface Research, Kantstr. 55, D-14513 Teltow, Germany.

0144-8617/98/$19.00
PII S0144-8617(98)00029-0

higher expansion and stiffness with increasing DA (Anthonsen et al., 1993, Anthonsen et al., 1994; Ottøy et al., 1996a), the opposite effect, namely higher compactness for molecules of a higher DA, has been described by Errington et al. (1993). These authors found a correlation between molar mass M_w (from sedimentation analysis) and intrinsic viscosity $[\eta]$ when the samples originated from the same parent material. Data for samples of different origin did not fit the same relationship. Terbojevich et al. (1991) and Rinaudo et al. (1993) could not confirm these findings. These workers found that the persistence length L_P as an expression for the chain stiffness does not depend on DA. However, their values given as $L_P = 5$ nm (Rinaudo et al., 1993) and $L_P = 22$ nm (Terbojevich et al., 1991), respectively, differ significantly. Both groups have derived their data from the relationship between molar mass M_w and radius of gyration $R_{g,z}$ using static light scattering (SLS) alone (Terbojevich et al., 1991) or in combination with size exclusion chromatography (MALLS–HPSEC) (Rinaudo et al., 1993). In interpreting their experimental results, excluded volume was considered but the polydispersity of the samples was not. Making additional assumptions, Rinaudo et al. (1993) have shown by calculation that their persistence length was also consistent with the Mark–Houwink exponent ($M_w^{0.76}$) obtained for the same series of fractions. A similar experimental approach by Beri et al., 1993 led to an exponent as low as $M_w^{0.2}$ (or even lower!) that cannot be conclusively explained. Possible reasons given by the authors were extremely poor chromatographic separation and/or branched admixtures. Applying static light scattering to concentration series, Anthonsen et al. (1994) obtained Zimm plots of a very anomalous shape. In the low concentration range, the apparent molar mass M_w increases with increasing concentration, giving negative B values which turn, eventually, to positive B values at higher concentrations. These plots were interpreted in terms of a concentration-dependent self-association. Wu et al. (1995) also mentioned that "... at higher concentration, chitosan, especially those samples with higher molecular weight, will form larger aggregates ...". This, however, is somehow surprising as none of the other techniques such as membrane osmometry (Anthonsen et al., 1993), ultracentrifugation (Errington et al., 1993), viscosity measurements (Anthonsen et al., 1993) and even SLS (Terbojevich et al., 1991; Wu et al., 1995) has provided any evidence for such processes when carried out under comparable conditions. The high second virial coefficients B reported by these workers (all of them in the order of magnitude of 10^{-3} ml mol g^{-2}, no matter which technique had been applied) are consistent with the theory for flexible linear polyelectrolytes (§27c in Tanford, 1965). Studying pectins we were faced with very similar problems (Berth et al., 1994). Based on this experience we propose that, in the case of chitosan, filtration effects upon clarification associated with the presence of some (undiscovered) particulate matter might be the reason for the distortions observed. This proposal is supported by the fact that changes in temperature and solvent did not substantially affect the shape of Zimm plots as the authors themselves stress (Anthonsen et al., 1994). Indeed, the presence of difficult to remove particles in chitosan solutions has already been observed in static light scattering (Domard and Rinaudo, 1983 — interpreted as the result of self-aggregation) and dynamic light scattering experiments (Wu et al., 1995). However, SLS measurements carried out simultaneously provided very sensible data such as $R_{g,z}$ (nm) = $2.4 \times 10^{-2} M_w^{0.64}$ and R_g/R_h ratios (R_h, hydrodynamic radius from dynamic LS) close to 2.0 for a set of samples with DA = 9% and a series of molar masses in 0.2 M acetic acid/0.1 M sodium acetate at room temperature.

In this present paper we report results on three commercial chitosans varying in DA obtained by membrane osmometry (M_n, B), viscometry ($[\eta]$), and static light scattering (M_w, $R_{g,z}$, B). In addition to investigations on the unfractionated parent samples, gel permeation chromatography (GPC) on Sepharose CL-2B was used for fractionation according to size in order to establish relationships between $[\eta]$ and M_w (Mark–Houwink–Kuhn–Sakurada equation) and $R_{g,z}$ and M_w. Based upon these data, the conformation of chitosan macromolecules in acetate buffer will be discussed.

Emphasis will be put on methodical aspects of SLS studies such as the effect of various conditions for clarification and the correction for polydispersity. The model for wormlike chains with excluded volume effect was used for the interpretation of data.

A requirement for light scattering studies is the preparation of optically clean polymer solutions to avoid any disturbance due to even very small amounts of large extraneous contaminations or supramolecular constituents of the substance studied (see, for example, the excellent presentation given by Tabor (1972)). For aqueous solutions, there are in principle only two methods of clarification to choose from: (i) filtration through membrane filters of carefully selected pore size, or (ii) the same as (i) in combination with a centrifugation step under controlled conditions. Whereas filtration alone is efficient in all cases where the undesired contamination is of large dimensions compared with the molecularly disperse polymer to be studied, the combination with centrifugation is recommended in situations where contaminations are of same size or size distribution but of greater compactness.

2. Experimental

2.1. Materials

Three commercial products were used without any prepurification or chemical modification. Chitosan A was delivered by 'fishcontract' (Bremerhaven, Germany). The DA was determined as DA = 25% by titration. The other

two samples were: (i) low-molecular weight chitosan (chitosan B); $[\eta]$, 120–160 ml g^{-1}; DA, 22.5%; water content 1.3–9.9%; and (ii) high-molecular weight chitosan (chitosan C); $[\eta]$, 1200–1400 ml g^{-1}; DA, 7%; water content 5.6–8.3%.

Acetate buffer of two ionic strengths were employed: (i) 0.02 M sodium acetate and 0.02 M acetic acid were mixed to give a pH of 4.5, and (ii) the same solutions but also containing 0.1 M NaCl were mixed to give a pH of 4.5.

Chitosan was dissolved at room temperature under slight shaking at least for 24 h. If indicated, solutions were ultracentrifuged (Beckman preparative ultracentrifuge L-70, fixed angle rotor Ti 70.1, 90 min, 40 000 rpm, 20–25°C). The supernatant was separated from the (colourless lens-like) precipitate using a syringe.

All membrane filters used were made of cellulose nitrate (Sartorius-Membranfilter-GmbH, Germany).

Polysaccharide concentrations were controlled by means of refractive index measurements (see below) after operations such as centrifugation or filtration (Brice Phoenix differential refractometer, UK).

2.2. Methods

2.2.1. Gel permeation chromatography

The GPC equipment consisted of a Pharmacia column (2.6 cm diameter, 95 cm length) filled with about 500 ml Sepharose CL-2B, a differential refractometer RID-6 (Shimadzu, Japan), a peristaltic pump (P1), a ReCyChrom valve for the sample injection and an UltroRac sample collector (all LKB Produkter, Sweden).

A sample volume of about 16 ml (~2 mg ml^{-1}) was injected into the ascending flow stream of about 15 ml h^{-1}. Degassed 0.02 M acetate buffer with 0.1 M NaCl, pH 4.5, was used as solvent and eluent. If not mentioned otherwise, the fractions of ~16 ml each were filtered directly (pore size, 0.45 μm) into the dust-free measuring cell in the reverse order of their appearance for off-line SLS and, afterwards, viscosity measurements.

2.2.2. Viscosity measurements

These were carried out in an Ubbelohde type (Schott-Geräte, Germany) capillary viscometer (Lauda, Germany) at 25.0°C. The flow time for pure water was nearly 8.5 s. The intrinsic viscosity was obtained by extrapolating η_{rel}/c to zero concentration (with c the polymer concentration in g ml^{-1}).

2.2.3. Membrane osmometry

Experiments were performed in 0.02 M acetate buffer/0.1 M NaCl, pH 4.5, at 30°C using a commercial osmometer (Osmomat 090, GONOTEC, Germany) equipped with two-layer membranes (cutt-off: ~5 kD, made of cellulose acetate, supplier: GONOTEC, Germany) and concentrations up to 0.25 g/100 g solvent. The number average molar mass was calculated according to $M_n = R(T/(\pi/c)_{c=0}$ where $(\pi/c)_{c=0}$ is the reduced osmotic pressure extrapolated to zero concentration (linear regression), R is the universal gas constant, and T the temperature. The osmotic second virial coefficient B was obtained from the slope of π/c versus c.

2.2.4. Static light scattering

Measurements were performed at 22–23°C in cylindrical cells using a SOFICA instrument (FICA, France), model 42000, equipped with a 5 mW helium/neon laser at an operating wavelength of $\lambda_0 = 632.8$ nm. The scattered light intensity was measured at 31 positions between 30 and 150°. The Zimm procedure (see Huglin, 1972) was used to derive M_w, $R_{g,z}$, and B by plotting Kc/R_θ versus $q^2 + kc$, where $q = (4\pi/\lambda)(\sin\theta)$ with θ the angle of observation, K the optical constant (see below), and k an arbitrary constant.

For the same wavelength, the specific refractive index increment on chitosan A was obtained as $\partial n/\partial c = 0.203$ ml g^{-1} in both solvents after equilibrium dialysis (Brice Phoenix differential refractometer, UK; cutt-off of the dialysis tube used: 5 kD). This value has been taken throughout this report for the calculation of the optical constant K.

3. Results and discussion

3.1. Studies on the unfractionated parent samples

Table 1 collects the results of membrane osmometry and viscometry in 0.02 M acetate buffer plus 0.1 M NaCl, pH 4.5. All three samples have shown good solubility, apart from a few 'clouds' of negligible mass, so that the original matter is entirely represented by these data. As to be expected, an increasing molar mass corresponds to increasing intrinsic viscosity. All B values obtained were of the order of 10^{-3} ml mol g^{-2} as described elsewhere (Anthonsen et al., 1993) irrespective of the DA. Simple linear dependencies of η_{red} and π_{red}, respectively, versus c allowed easy extrapolation and the parameters obtained had a high level of precision. In contrast, at low ionic strength (I = 0.02 mol l^{-1}) η_{red} increased with decreasing polymer concentration so that most of our studies were performed in the higher ionic strength NaCl containing buffer (I = 0.12 mol l^{-1}). The manufacturer's intrinsic viscosity data were confirmed only for chitosan B. Our value for chitosan

Table 1
Results of viscometry and membrane osmometry: solvent, 0.02 M acetate buffer/0.1 M NaCl, pH 4.5

Sample	DA (%)	$[\eta]$ (ml g^{-1})	M_n (g mol^{-1})	$B_{osm} \times 10^3$ (ml mol g^{-2})
Chitosan A	25	333	31075	4.92
Chitosan B	22.5	150	20400	9.50
Chitosan C	7	650	57400	6.76

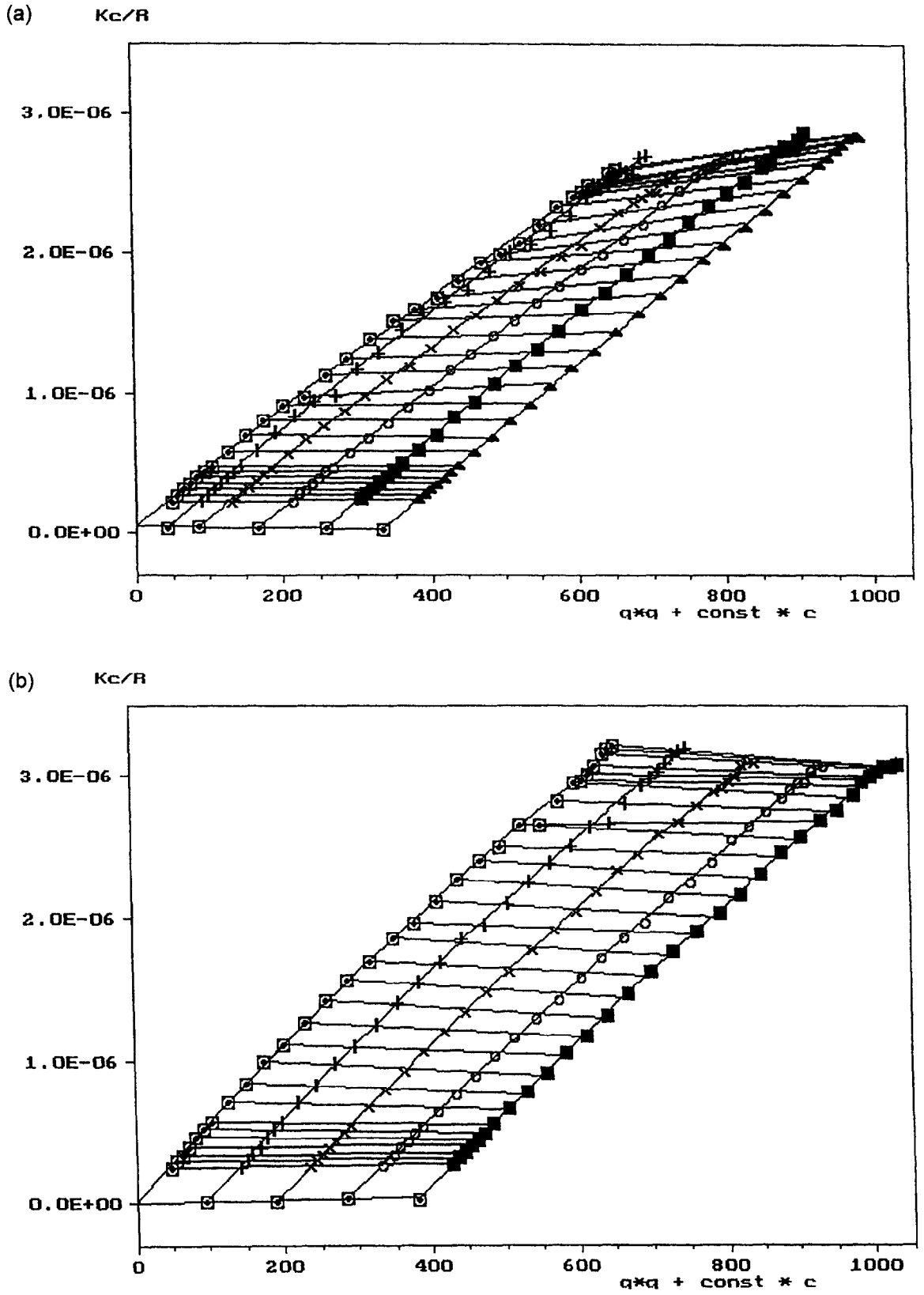

Fig. 1. Zimm plots for chitosan A at various ionic strengths (8.0 μm pore size used for clarification). (a) 0.02 M acetate buffer, pH 4.5; $M_w = 1.99 \times 10^7$ g mol^{-1}, $R_{g,z} = 509$ nm, $B = -1.107 \times 10^{-8}$ ml mol g^{-2}. (b) 0.02 M acetate buffer/0.1 M NaCl, pH 4.5; $M_w = 2.6 \times 10^8$ g mol^{-1}, $R_{g,z} = 2113$ nm, $B = 1.6 \times 10^{-8}$ ml mol g^{-2}.

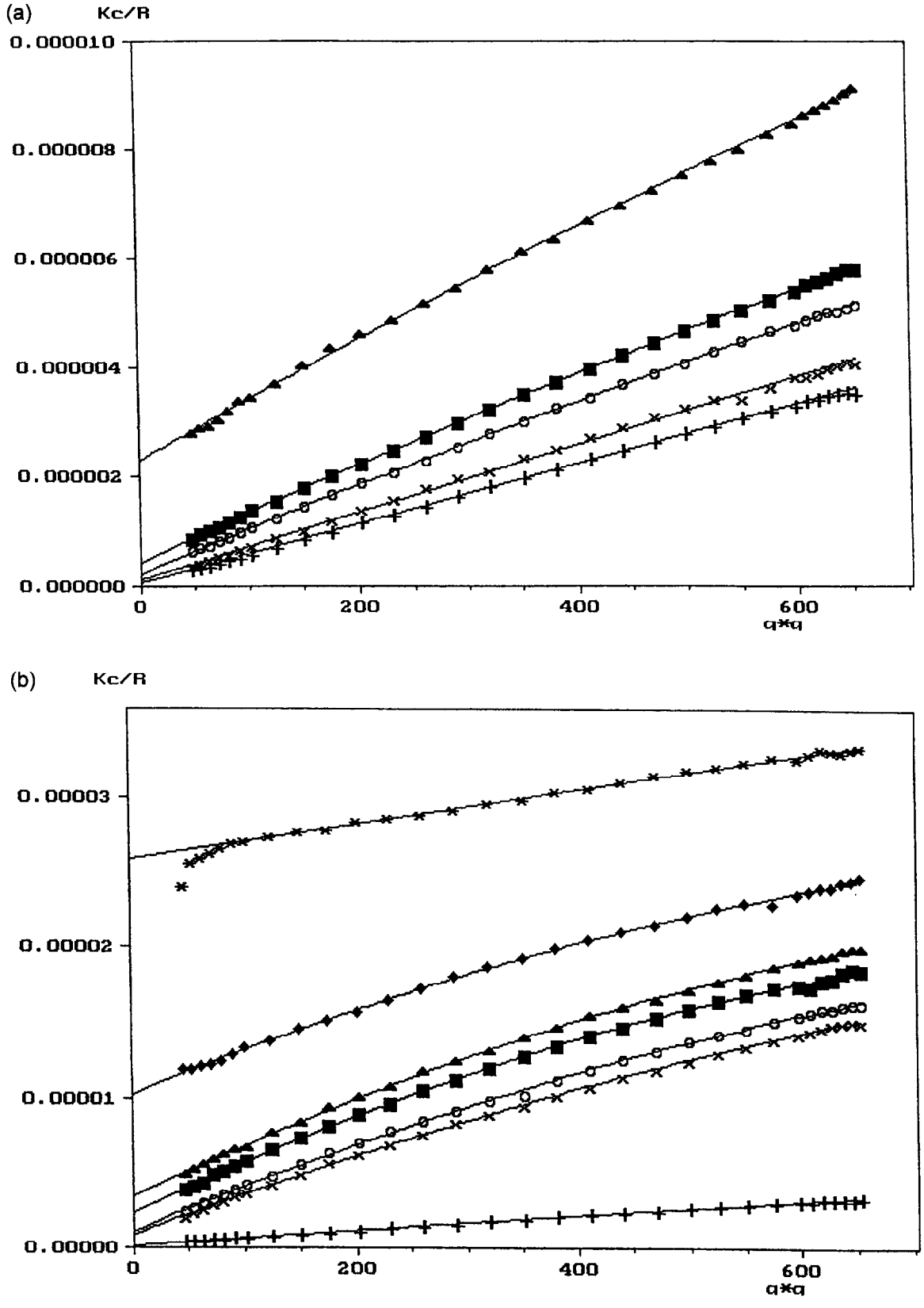

Fig. 2. Zimm plots for the filtration tests: effects of successive reduction of the pore size of membrane filters used for clarification (for details, see also Table 2). (a) Original solution, pore size (μm): +, 8.0; × 5.0; □, 1.2; ■, 0.8; ▲, 0.45. (b) Supernatant of ultracentrifugation, pore size (μm): +, 8.0; × 8.0; after centrifugation: □, 5.0; ■, 1.2; ▲, 0.8; ◆, 0.45; *, 0.2.

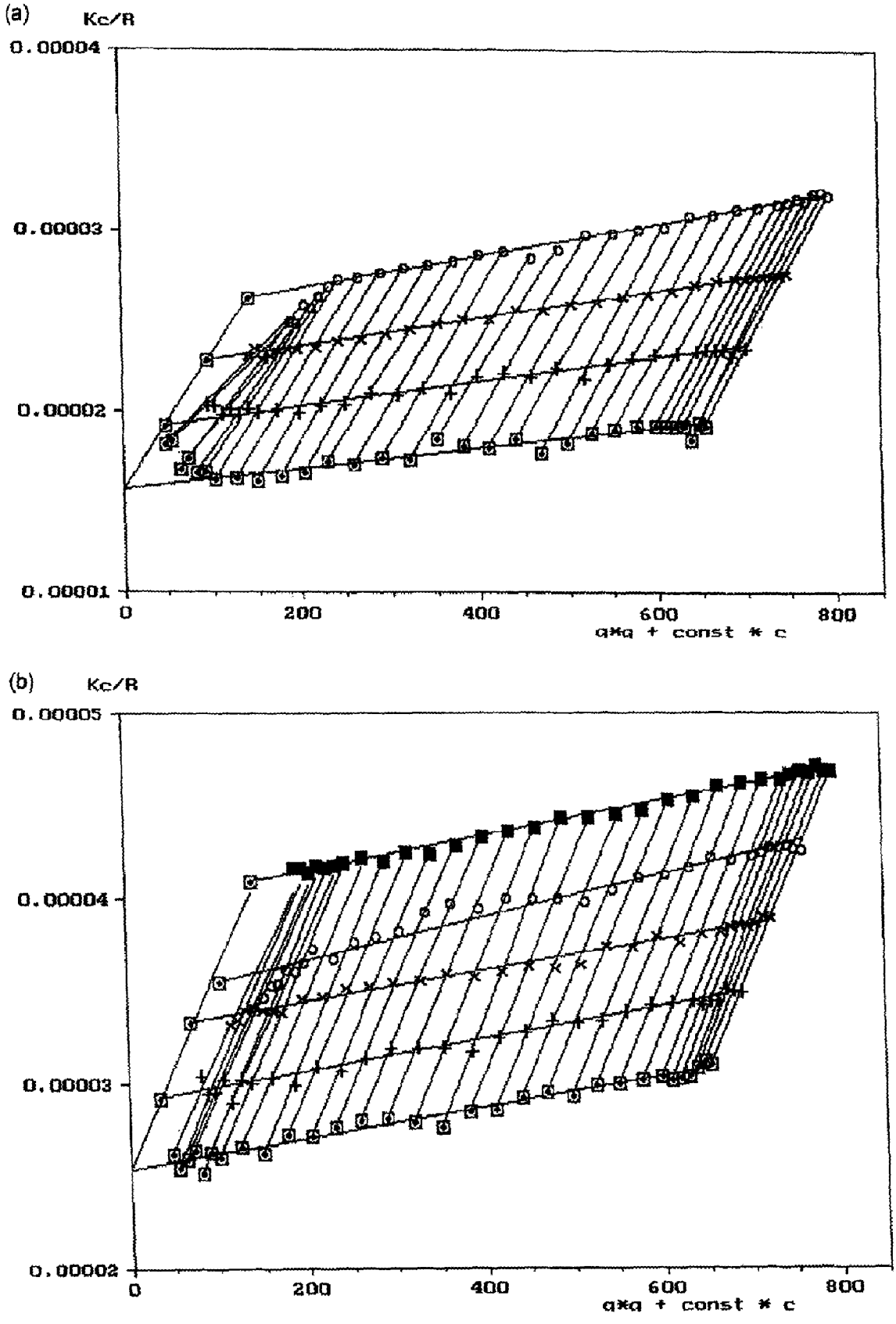

Fig. 3. Zimm plots for chitosana in 0.02 M acetate buffer/0.1 M NaCl, pH 4.5: (a) chitosan A (0.2 μm), (b) chitosan B (0.2 μm), (c) chitosan C (0.45 μm).

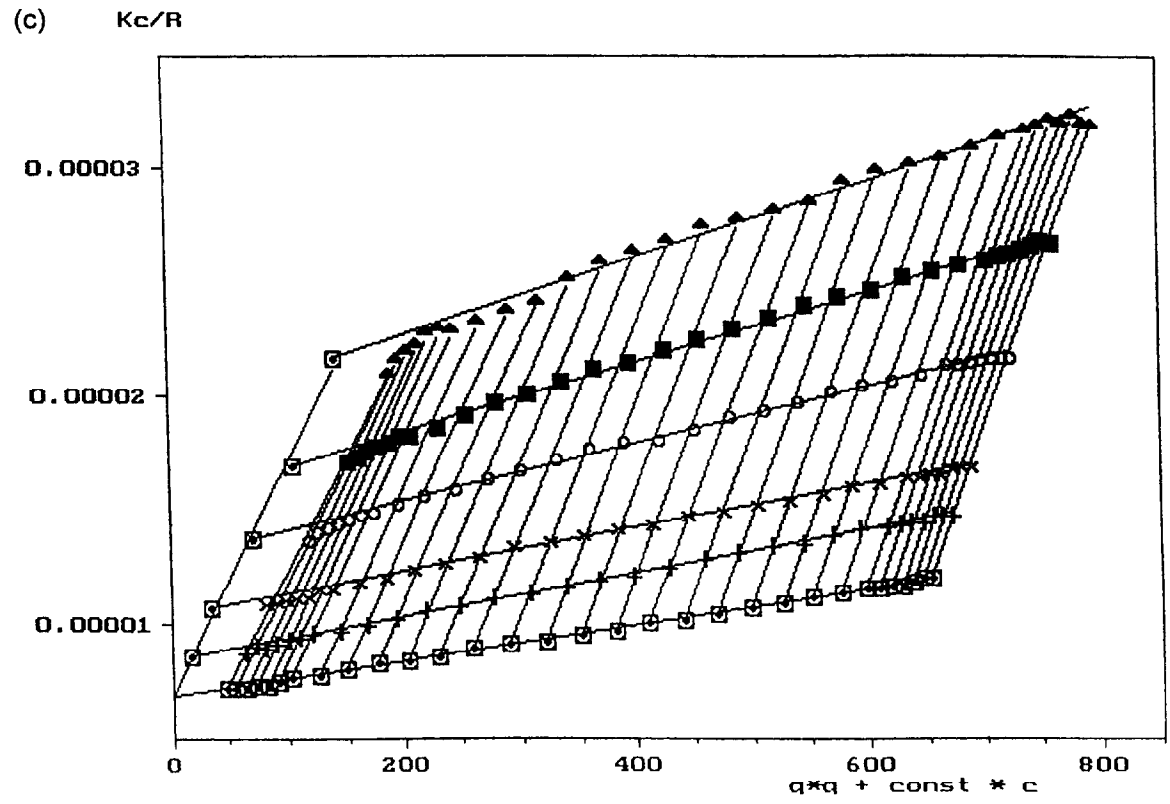

Fig. 3. Continued.

C was much lower than theirs. Unfortunately, no information on how the latter data had been determined was available.

Fig. 1 presents Zimm plots for chitosan A for the two ionic strengths above. Stock solutions of about 1 mg ml^{-1} were filtered once through a 8.0 μm pore size membrane. The concentration series was then prepared and each sample was filtered through the same pore size filter directly into the measuring cells in order of increasing concentration. Extremely high molar masses M_w as well as extremely low virial coefficients (given in the legend) — when considered in the context of the data from osmometry and Huggins constants of about 0.4 — indicate that the scattering behaviour of the sample as a whole is dominated by large particles for which

Table 2
Results of filtration tests on chitosan A (see Fig. 2): solvent, 0.02 M acetate buffer/0.1 M NaCl, pH 4.5

	Original solution (c_{stock} = 1.77 mg ml^{-1})			Supernatant from ultracentrifugation (c_{stock} = 1.94 mg ml^{-1})		
Pore size (μm)	c (mg ml^{-1})	$M_{w,app} \times 10^{-5}$ (g mol^{-1})	$R_{g,z}$ (nm)	c (mg ml − 1)	$M_{w,app} \times 10^{-5}$ (g mol^{-1})	$R_{g,z}$ (nm)
8.0	1.77	231	615	1.83	11.9	319
5.0	1.76	77.8	379	1.82	9.47	299
1.2	1.75	44.3	335	1.82	4.35	216
0.8	1.70	22.8	252	1.81	2.95	78
0.45	1.68	4.37	122	1.81	0.98	94
0.2	n.d.	n.d.	n.d.	1.80	0.39	37

Table 3
Results of characterization by static light scattering (alone and in combination with GPC)

Sample	M_w (g mol^{-1})	$B_{SLS} \times 10^3$ (ml mol g^{-2})	$R_{g,z}$ (nm)	M_{GPC} (g mol^{-1})	M_w/M_n	σ	M_L (g mol^{-1} nm^{-1})	L_w (nm)	α	$\langle R_{g,\theta}\rangle_z$ (nm)	L_P (nm)	$B_{calc} \times 10^3$ (ml mol g^{-2})
Chitosan A	63830	3.55	33.0	60000	2.05	0.85	349	182	1.18	27.9	6.5	7.4
Chitosan B	39260	3.88	31.4	36200	1.92	0.81	347	113	1.13	27.7	12.5	8.2
Chitosan C	147000	6.76	59.3	184000	2.56	0.97	335	439	1.26	47.1	6.0	6.6

$B \sim 0$. For that reason we had to deal with the problem of clarification following previous experience on other polysaccharides (Berth et al., 1994, Berth et al., 1996a, Berth et al., 1996b). The effectiveness of membrane filtration by itself as well as after ultracentrifugation was checked. As shown previously, studies were carried out as single-concentration series (initial concentration about 2 mg ml^{-1}). Starting with a pore size of 8.0 μm, pore size was reduced successively (three repetitions at each pore size level) via 5.0, 1.2, 0.8, to, finally, 0.45 μm (all without centrifugation) or 0.2 μm (after centrifugation), respectively. A pore size of 0.2 μm could not be applied in the case of the uncentrifuged solution (Fig. 2(a)) because the membrane blocked almost immediately. The loss in concentration was followed by measuring the refractive index. All in all, not more than 3–7% of the dried original matter disappeared as result of clarification. This is negligible compared with the loss in the scattering intensity as can be seen from the Zimm plots in Fig. 2 (observe the different ordinate scales) whereas the correspondingly checked flow times in the capillary viscometer remained unchanged within experimental error. This is seen to indicate the selective removal of particulate material. In Table 2, the effects of solution treatment in terms of apparent molar masses and radii of gyration (from a linear or quadratic fit) are given. It is obvious that the effect of filtration became more important for the centrifuged stock solution as the pore size decreases. These findings suggest the presence of particulate matter of a broad size distribution in the original sample. That is why a combination of centrifugation and filtration is considered to be the method of choice. Similar results were obtained in the low ionic strength buffer so that the choice of ionic strength is not believed to fundamentally change the situation. At each level of clarification, solutions revealed a stable scattering behaviour at least over a few days when stored at room temperature.

Based upon our clarification experiments, we obtained Zimm plots for the three chitosan samples under study as shown in Fig. 3(a)–3(c) when the following somewhat cumbersome procedure had been applied. The sample was dissolved in the corresponding volume of freshly filtered buffer (same pore size as finally used; stock solution $c_0 \sim 2$ mg ml^{-1}) for 24 h. The stock solution was centrifuged (details above), filtered at least three times at each pore size level downward (just as used to obtain the data in Fig. 2) until the desired pore size was reached. Then the concentration series was prepared by adding freshly filtered buffer (weight control) and, finally, the solutions were filtered directly into the measuring cells in order of increasing concentration (blank solvent first). The finally chosen pore size was dependent on the sample (see the legend to Fig. 3). It is worth mentioning that the omission of filtration steps within the series reduced the reproducibility and quality of the resultant Zimm plots. The parameters extracted from Fig. 3 are collected in Table 3.

If filtration through a 0.2 μm filter is omitted, the Zimm

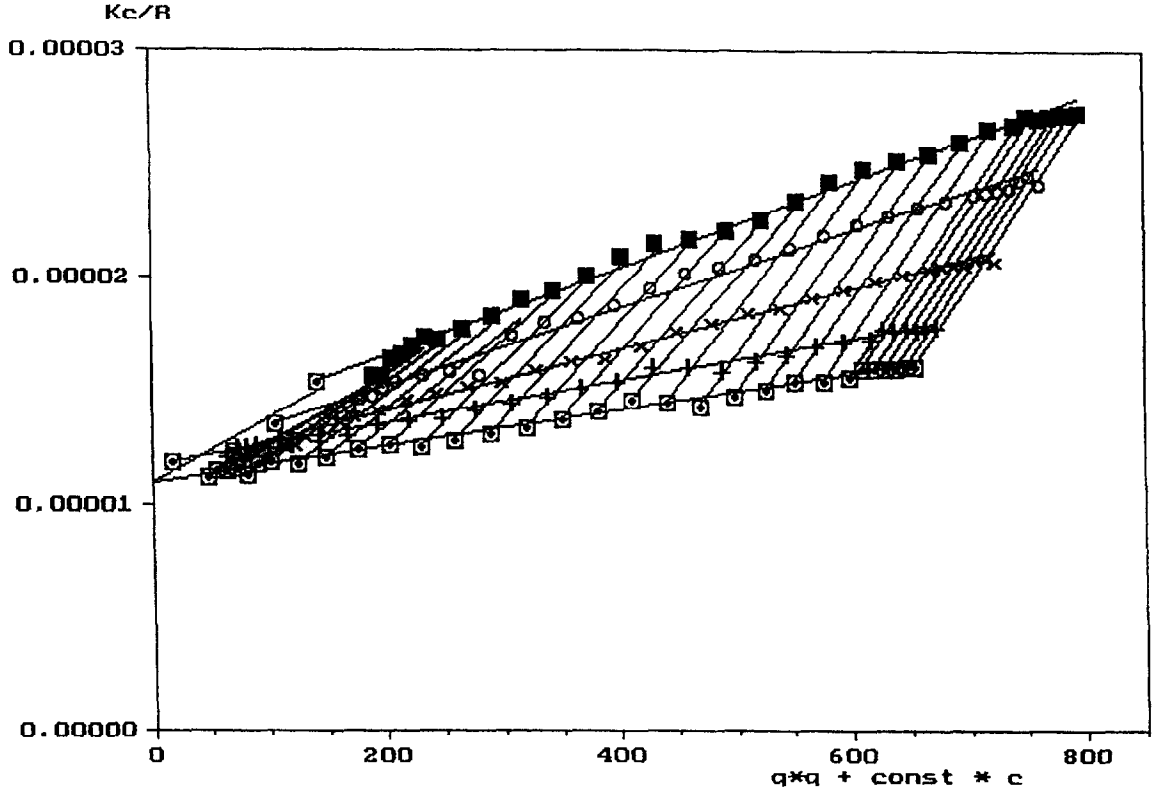

Fig. 4. Zimm plot for chitosan A (supernatant) after "less severe" clarification (0.45 μm). $M_w = 91\,930$ g mol^{-1}, $R_{g,z} = 47$ nm; $B = 1 \times 10^{-3}$ ml mol g^{-2}.

plot in Fig. 4 for chitosan A was obtained. It not only gives the expected higher average molar mass but is also distorted in a way which is indicative of increasing proportions of higher molar mass species with increasing polymer concentration. As pointed out for pectins (Berth et al., 1994) and reviewed by Lee (1993) this may well be an effect of filtration caused by the presence of small amounts of particulate matter. From Fig. 3(a) and Fig. 4 it follows that, once removed, particles were not reformed which does not support the idea of a concentration dependent association.

At first glance, the parameters in Table 3 appear to be reasonably consistent with the data in Table 1. For their further interpretation in terms of a polydisperse system of wormlike chains with excluded volume effect, the following approach has been used (see, for example, Chapter 5 in Dautzenberg et al. (1994)).

In a monodisperse system of wormlike chains, the radius of gyration under θ conditions, $R_{g,\theta}$, is related to the persistence length L_P according to Eq. (1) with L, the contour length.

$$R^2_{g,\theta} = \frac{LL_P}{3} - L_P^2 + \frac{2L_P^3}{L} - \frac{2L_P^4}{L^2}(1 - e^{-L/L_P}) \quad (1)$$

For polydisperse systems, light scattering provides the z-average of the radius of gyration $\langle R^2_{g,\theta}\rangle_z$ which can be written as

$$\langle R^2_{g,\theta}\rangle_z = \frac{1}{L_w}\int_0^\infty LR^2_{g,\theta}(L)p_w(L)\,dL \quad (2)$$

with $p_w(L)$ the normalized weight distribution of contour lengths, and L_w the weight average contour length, which is given as $L_w = M_w/M_L$, with M_L the mass per unit length. The polydispersity parameter is determined by M_w/M_n and

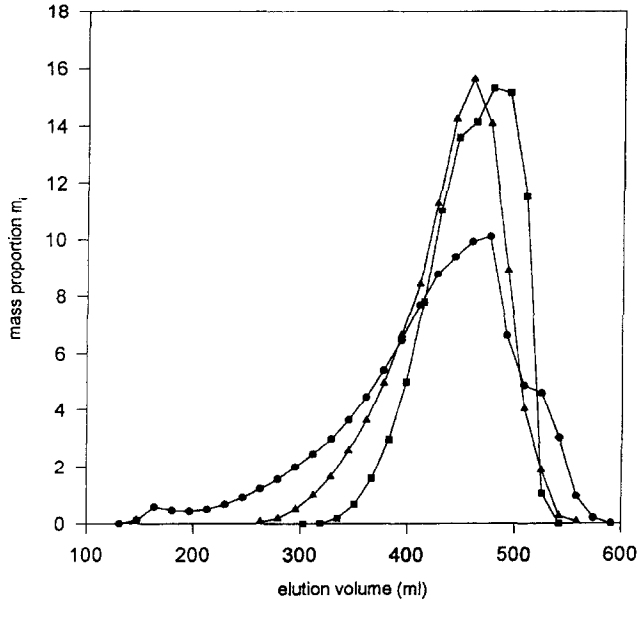

Fig. 5. Normalized elution lines ($\Sigma m_i = 1$) of the three chitosan samples on Sepharose CL-2B (V_o ca. 135 ml, V_t ca. 550 ml): ●, chitosan C; ▲, chitosan A; ■, chitosan B.

the type of distribution. Using a logarithmic distribution (Dautzenberg and Rother, 1992), the polydispersity σ is defined as $M_w/M_n = e\delta^2$. Knowing L_w, L_P can be estimated by fitting $\langle R^2_{g,\theta}\rangle_z$ using Eqs. (1) and (2).

Having measured the radius of gyration in a good solvent — this means far from θ conditions ($B_{exp} \gg B_\theta = 0$) — R^2_g can be converted to $R^2_{g,\theta}$ using $R^2_g = \alpha^2 R^2_{g,\theta}$ with α the expansion factor. Following Flory, α can be expressed as $\alpha^5 - \alpha^3 = (134/105)z$ where the z parameter is related to the excluded volume β

$$z = \left(\frac{3}{2\pi l_K^2}\right)^{3/2} \beta N_K^{1/2} \quad (3)$$

with l_K the Kuhn length ($l_K = 2L_P$) and N_K, the number of Kuhn segments per chain ($N_K = L/l_K$). For highly charged polyelectrolytes (charge distance $b < \lambda_B$; λ_B, Bjerrum length) with hydrophobic backbones, the electrostatic term of the excluded volume is dominant which is given by Odijk and Houwaart (1978) as

$$\beta_{el} = 8\pi\lambda_D L_P^2 \quad (4)$$

Herein λ_D is the Debye–Hückel screening length which depends on the ionic strength I of the solvent according to

$$\lambda_D = \left(\frac{1000}{8\pi\lambda_B N_A I}\right)^{1/2} \quad (5)$$

if the ionic strength is given in mol l^{-1} and λ_B, λ_D in centimetres. With λ_B, the Bjerrum length, as 7 Å in water at room temperature, and N_A as Avogadro's number, λ_D = 8.87 Å comes out for I = 0.12 mol l^{-1}.

Starting with a persistence length obtained from Eqs. (1) and (2) and neglecting the excluded volume effect, one can calculate β_{el}, z_{el}, and α to a first approximation, which leads to refined values of $\langle R^2_{g,\theta}\rangle_z$ and L_P. An iterative procedure yields finally the correct values for α, $\langle R^2_{g,\theta}\rangle_z$, and L_P. To calculate M_L, an average monomer weight (taking into account the various DA) was taken. The length per monomer unit was assumed to be 4.9 Å by analogy to other polysaccharides. The resulting data for α, $\langle R^2_{g,\theta}\rangle_z^{1/2}$ and L_P are given in Table 3. It shows almost identical L_P values for chitosan A (DA~25%) and chitosan C (DA~7%) whereas chitosan B (DA~22%) seems to drop out of the series. We feel that, in view of the very limited amount of data, this deviation should not be overvalued. They are likely to reflect the experimental problems discussed in detail above. In any case, our values are relatively close to those published by Rinaudo et al. (1993) but would have been much higher without taking into account the effect of polydispersity (see below).

Having determined data for the molar mass M, the persistence length L_P, the excluded volume β and the z parameter, one can also predict the second virial coefficient B according to

$$B = \frac{N_A N_K^2 \beta}{2M^2} h(z) \quad (6)$$

with $h(z) = 1/(5.73z)\ln(1 + 5.73z)$. The predicted values

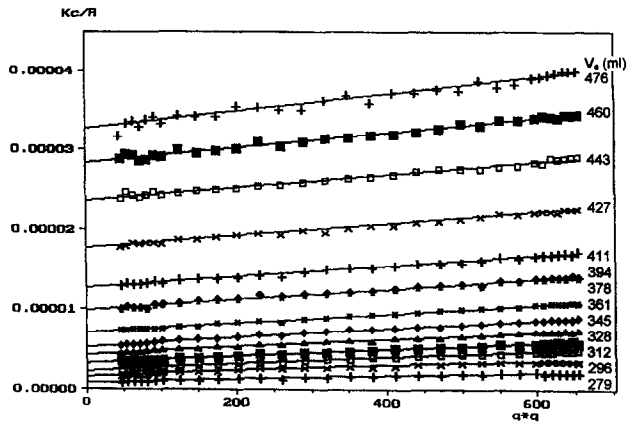

Fig. 6. Zimm plot for the fractions of chitosan A according to Fig. 5. V_e, elution volume at GPC.

(Table 3) are all of the order of 10^{-3} ml mol g^{-2} and, on average, only slightly higher than those found experimentally.

3.2. Studies on GPC fractions

The same chitosan samples as above were fractionated on Sepharose CL-2B. The elution patterns are shown in Fig. 5. No loss in material by absorption was noticed confirming the findings of others (Ottøy et al., 1996b). The fractions were taken for off-line SLS (after filtration through a 0.45 μm pore size membrane directly into the measuring cell) and the viscosity was measured at the concentration given by GPC. Fig. 6 shows the SLS measurements for the fractions which are used for the $[\eta]$–M_w relation (Fig. 7) as well as the $R_{g,z}$–M_w relation (Fig. 8). Taking an average second virial coefficient of $B = 4 \times 10^{-3}$ ml mol g^{-2} (Table 3), the measured curves were extrapolated to zero concentration according to $Kc/R(\theta)_{c=0} = Kc/R(\theta) - 2Bc$ which was found to increase the apparent molar masses by up to 15%. The concentration dependence of the reduced viscosity was neglected as the error did not exceed 3% even at the highest concentrations in the eluent (Huggins constant k_H as 0.4).

Fig. 7 collects $[\eta]$ and M_w data for GPC fractions from all three samples and several GPC runs. The M_w data cover a range from about 10^4 to 10^7 g mol^{-1}. (Plotting $[\eta]$ versus DP instead modifies the plot only slightly as the difference in monomer unit weights according to DA does not exceed 4.1%.) The majority of points were found to lie on a slightly curved line with slopes for tangents between 1.0 in the low molecular weight region and about 0.5 in the high molecular weight domain. The individual curves reveal, for increasing molar masses, a levelling off or even a downward curvature. This is indicative of increasingly compact structures with increasing molar mass but can be caused as well by growing proportions of increasingly compact species (two-component systems). The behaviour of chitosan B is notable. At a given intrinsic viscosity, M_w was found to be distinctly higher for this sample almost over the whole range of molar masses. Considering the whole set of samples and fractions, one gets the impression that both higher molar masses at the top of the distribution for each population and a higher degree of acetylation even for relatively low-molecular products can result in the occurrence of relatively compact species. Bearing in mind that chitosans are partly de-acetylated and degraded chitins whose solubility depends on DA and molar mass (Vårum et al., 1994; Kubota and Eguchi, 1997), we propose that these more compact species may well be a residue from the biological source, i.e. imperfectly de-acetylated and less degraded ('chitin-like') fractions in a heterogeneous population. This is consistent with observations of Vikhoreva et al. (1996) who found between 5 and 15% by weight with a distinctly higher DA compared with the bulk of the samples with a relatively low DA (ca. 20%) when a solid-phase procedure had been used for deacetylation (see also Ottøy et al., 1996a). Indeed, the conditions for deacetylation and subsequent processing of products are expected to be of great importance both in determining the (molecular) features of the final product and in the field of application. (Varying heterogeneity could possibly explain why analytical ultracentrifugation has led to different compactness of molecules despite the same average degree of acetylation (Errington et al., 1993).) The combined filtration and centrifugation clarification procedure is not for all chitosans as effective as we would like it to be, taking into account the concentration-dependent effects upon clarification on some samples. Thus there is no need to assume that these particulate species had been molecularly dispersed previously. Similar ideas might have prompted the determination of the DA along the molar mass distribution by Ottøy et al., 1996b but no trend has been

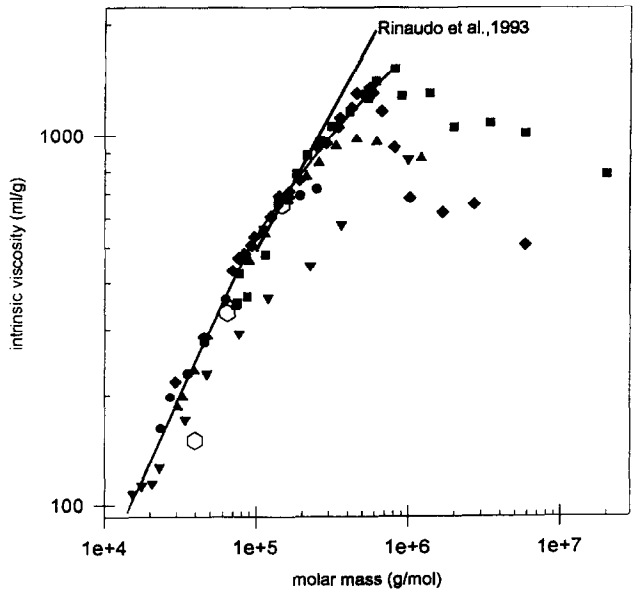

Fig. 7. $[\eta]$–M_w plot obtained for fractions from several GPC runs for the samples according to Fig. 5: ●, ▲, chitosan A; ■, ◇, chitosan C; ▼, chitosan B; ○, parent samples.

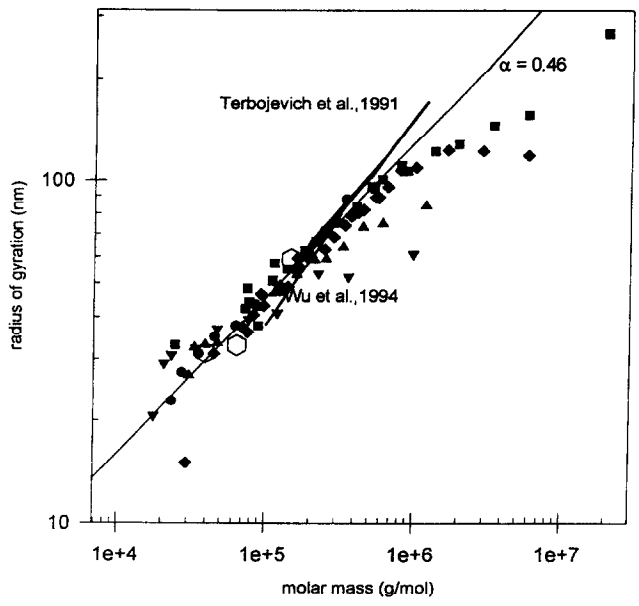

Fig. 8. $R_{g,z}$–M_w plot for the fractions from GPC runs according to Fig. 5 and Fig. 6 (for symbols, see Fig. 7).

noticed. However, it is likely to be very difficult to prove such trace amounts in terms of chemical composition as even their total removal will not markedly affect the average for the remainder.

Returning to Fig. 7, we would like to stress that our [η]–M_w relation is very close to that established by Rinaudo et al., 1993 despite a somewhat different solvent. Two of our values obtained on the unfractionated samples (Tables 1, and 3) fit their straight line (derived for $10^5 < M_w < 6 \times 10^5$) perfectly. Moreover, summing up the individual molar masses of the fractions according to their mass proportions, we obtain the average values in Table 3 which are in acceptable agreement with those estimated for the parent samples (Table 3).

Finally, the plot for $R_{g,z}$ versus M_w is given in Fig. 8. Again, the majority of the values forms a unique line covering a molar mass range from 25 000 to a million with a slope as low as 0.46 irrespective of DA. $R_{g,z}$ as a function of M_w reveals the same tendency as to level off at high M_w as does [η]. The corresponding (average) data for the parent samples from Table 3 fit the line quite well. This might be one way to illustrate the consistency of our data. However, the slope of nearly 0.5 in our $R_{g,z}$–M_w relation which is indicative of Gaussian coils ($R_g \sim M_w^{0.5}$) rather than wormlike chains with excluded volume effect ($R_g \sim M_w^{0.6}$) remains to be explained. Studying very stiff macromolecules such as xanthan (Berth et al., 1996a) and xylinan (Berth et al., 1996b) in the same way (GPC plus SLS), we were confronted with a very similar problem. It could be resolved by model calculations making use of the wormlike chain model. It has been shown that an increasing polydispersity of the fractions with increasing elution volume could explain the experimental data. Unlike the present situation with chitosan, for these polymers the number of Kuhn segments per chain was small ($N_K \leq 5$) so that no excluded volume effect had to be taken into account. Following in principle the same strategy but

Table 4
Results of model calculations on GPC fractions for the three chitosans varying in degree of acetylation, LP = 6.2 nm (for symbols and elution volumes, see Fig. 5)

Sample (symbol)	Elution volume (ml)	M_w (g mol^{-1})	$R_{g,z}$ (nm)	L_w (nm)	z	α	$\langle R_{g,\theta}\rangle_z$ (nm)	M_w/M_n
▲	328.4	2.323e5	64.2	952	1.30	1.31	49.0	1.25
▲	344.8	2.545e5	59.3	729	1.14	1.29	46.0	1.43
▲	361.2	2.116e5	58.9	606	1.04	1.28	46.0	1.73
▲	377.7	1.612e5	53.0	462	0.90	1.26	42.1	1.90
▲	394.1	1.144e5	47.1	328	0.76	1.23	38.3	2.21
▲	410.5	8.917e4	42.7	256	0.67	1.21	35.3	2.42
▲	426.9	6.358e4	37.7	182	0.57	1.19	31.7	2.77
▲	443.3	4.726e4	33.5	135	0.49	1.18	28.4	3.01
■	366.5	2.249e5	53.5	648	1.07	1.28	41.8	1.34
■	382.4	1.192e5	41.2	344	0.78	1.23	33.5	1.63
■	398.4	4.645e4	39.4	220	9.62	1.20	32.8	2.47
■	414.3	4.712e4	36.9	136	1.49	1.18	31.3	3.67
■	430.2	3.689e4	32.3	98	0.42	1.16	27.8	4.02
■	446.2	2.345e4	30.9	67	0.34	1.14	27.1	5.71
●	230.0	8.064e5	107	2407	2.06	1.40	76.4	1.18
●	246.4	6.641e5	96.0	1982	1.87	1.38	69.5	1.19
●	279.2	5.531e5	89.5	1651	1.71	1.36	65.8	1.28
●	312.1	4.198e5	81.1	1253	1.49	1.34	60.5	1.43
●	344.9	3.422e5	74.3	1021	1.34	4.32	56.3	1.53
●	361.4	2.869e5	68.7	856	1.23	1.30	52.8	1.61
●	394.2	1.908e5	59.8	570	1.00	1.27	47.0	1.90
●	443.5	1.569e5	55.0	468	0.91	1.26	43.7	2.02
●	492.8	9.663e4	43.2	288	0.71	1.22	35.4	2.17
●	542.0	7.536e4	36.1	225	0.63	1.20	30.1	2.03

combining a wormlike chain model with excluded volume and the persistence length $L_P = 6.2$ nm (taken as average value for chitosan A and chitosan C from Table 3), we used the same set of equations given above in order to calculate β_{el} (Eq. (4)), the z-parameter (Eq. (3)), α, and, finally, $\langle R^2_{g,\theta}\rangle^{1/2}_z$ (Table 4). Then, assuming a logarithmic distribution again, the polydispersity σ was obtained by means of Eqs. (1) and (2) which can easily be turned into the M_w/M_n values which are also given in Table 4. The increase in M_w/M_n with increasing elution volume appears to be quite reasonable in context with our own results on other polysaccharides as well as general experience in the field of GPC. Thus, results from SLS, membrane osmometry, and GPC plus SLS are consistent with each other and the assumptions made for the interpretation of data seem to be justified. Very good agreement regarding the measured $R_{g,z}$–M_w relations exists also with findings published by Terbojevich et al., 1991 and Wu et al., 1995 at least in the upper range of molar masses.

The characterization of chitosan by means of hydrodynamic techniques such as dynamic light scattering and analytical ultracentrifugation will be the subject of further reports.

Acknowledgements

GB thanks Professor Markus Antonietti for the opportunity to realize this project in his department. Furthermore, the Deutsche Forschungsgemeinschaft (DFG) as well as the WELLA AG, Germany, are thanked very much for financial support and interest in this study. M. Struszczyk (Universität Potsdam) is thanked for the determination of the degree of acetylation. MGP acknowledges financial support given by the Fonds der chemischen Industrie, Germany.

References

Anthonsen, M.W., Vårum, K.M., & Smidsrød, O. (1993). Solution properties of chitosans: conformation and chain stiffness of chitosans with different degress of N-acetylation. *Carbohydr. Polym., 22*, 193–201.

Anthonsen, M.W., Vårum, K.M., Hermansson, A.M., Smidsrød, O., & Brant, D. (1994). Aggregates in acidic solutions of chitosans detected by static laser light scattering. *Carbohydr. Polym., 25*, 13–23.

Beri, G.B., Walker, J., Reese, E.T., & Rollings, J.E. (1993). Characterization of chitosans via coupled size-exclusion chromatography and multi-angle laser light scattering technique. *Carbohydr. Res., 238*, 11–26.

Berth, G., Dautzenberg, H., Christensen, B.E., Harding, S.E., Rother, G., & Smidsrød, O. (1996a). Static light scattering studies on xanthan in aqueous solutions. *Macromolecules, 29*, 3491–3498.

Berth, G., Dautzenberg, H., Christensen, B.E., Rother, G. & Smidsrød, O. (1996b). Physico-chemical studies on xylinan (acetan). Part I. Characterization by GPC on Sepharose CL-2B coupled with static light scattering and viscometry, Part II. Characterization by static light scattering. *Biopolymers, 39*, 709–719, 720–728.

Berth, G., Dautzenberg, H. & Rother, G. (1994). Static light scattering applied to pectin in dilute solution. Part I. Reliability of experiments and model calculations; Part II. The effects of clarification. *Carbohydr. Polym., 25*, 177–185, 187–195.

Dautzenberg, H., Jaeger, W., Koetz, J., Philipp, B., Seidel, C. & Stscherbina, D. (1994). *Polyelectrolytes—formation, characterization and application*. Munich: Hanser Publ.

Dautzenberg, H., & Rother, G. (1992). Supermolecular structures in polymer solutions. Interpretation of static light scattering data. *Makromol. Chem., Makromol. Symp., 16*, 94–113.

Domard, A., & Rinaudo, M. (1983). Preparation and characterization of fully deacetylated chitosan. *Int. J. Biol. Macromol., 5*, 49–52.

Errington, N., Harding, S.E., Vårum, K.M., & Illum, L. (1993). Hydrodynamic characterization of chitosans varying in degree of acetylation. *Int. J. Biol. Macromol., 15*, 113–117.

Huglin, M.B. (Ed.). (1972). *Light scattering from polymer solutions*. London: Academic Press.

Hunkeler, D. (1997). Polymers for bioartificial organs. *Trends Polym. Sci., 5*, 186.

Kubota, N., & Eguchi, Y. (1997). Facile preparation of water-soluble N-acetylated chitosan and molecular weight dependence of its water-solubility. *Polym. J., 29*, 123–127.

Lee, S. (1993). Determination of gel content in polymers. *Trends Polym. Sci., 1*, 303–309.

Odijk, T., & Houwaart, A.C. (1978). On the theory of the excluded volume effect of a polyelectrolyte in a 1–1 electrolyte solution. *J. Polym. Sci., Polym. Phys. Ed., 16*, 627.

Ottøy, M.H., Vårum, K.M., & Smidsrød, O. (1996). Compositional heterogeneity of heterogeneously deacetylated chitosans. *Carbohydr. Polym., 29*, 17–24.

Ottøy, M.H., Vårum, K.M., Christensen, B.E., Anthonsen, M.W., & Smidsrød, O. (1996). Preparative and analytical size-exclusion chromatography of chitosans. *Carbohydr. Polym., 31*, 253–261.

Peter, M.G. (1995). Applications and environmental aspects of chitin and chitosan. *J. Macromol. Sci., Pure and Appl. Chem., A32*, 629–640.

Rinaudo, M., Milas, M., & Dung, P.L. (1993). Characterization of chitosan. Influence of ionic strength and degree of acetylation on chain expansion. *Int. J. Biol. Macromol., 15*, 281–285.

Tabor, B.E. (1972). Preparation and clarification of solutions. In M.B. Huglin (Ed.), *Light scattering from polymer solutions*. London: Academic Press.

Tanford, Ch. (1965). *Physical chemistry of macromolecules* (3rd ed). New York: Wiley.

Terbojevich, M., Cosani, A., Conio, G., Marsano, E., & Bianchi, E. (1991). Chitosan: chain rigidity and mesophase formation. *Carbohydr. Res., 209*, 251–260.

Vikhoreva, G.A., Rogovina, S.Z., Akopova, T.A., Zelenetski, S.N., & Galbraikh, L.S. (1996). Fractional composition of chitosan obtained by solid-phase and suspension methods. *Vysokomol. Soedin. Ser., A38*, 1781–1785.

Vårum, K.M., Ottøy, M.H., & Smidsrød, O. (1994). Water-solubility of partially N-acetylated chitosans as a function of pH: effect of chemical composition and depolymerisation. *Carbohydr. Polym., 25*, 65–70.

Wu, C., Zhou, S.Q., & Wang, W. (1995). A dynamic laser light-scattering study of chitosan in aqueous solution. *Biopolymers, 35*, 385–392.